Anthropogenic Influence on the Rhine water temperatures

Alex Zavarsky[1] and Lars Duester[1]

[1]Federal Institute of Hydrology, Department G4- Radiology and Monitoring, Koblenz Germany

Correspondence: Alex Zavarsky (alexz@mailbox.org)

Abstract. River temperature is an important parameter for water quality and an important variable for physical, chemical and biological processes. River water is also used by production facilities as cooling agent. We introduce a new way of calculating a catchment-wide air temperature and regressing river temperature vs air temperatures. As a result the meteorological influence and the anthropogenic influence can be studied separately. We apply this new method at four monitoring stations (Basel, Worms, Koblenz and Cologne) along the Rhine and show that the long term trend (1979-2018) of river water temperature is, next to the increasing air temperature, mostly influenced by decreasing nuclear power production. Short term changes on time scales < 5 years are due to changes in industrial production. We found significant positive correlations for this relationship.

1 Introduction

River water temperature (T_w) greatly influences the most important physical, chemical and ecological processes in rivers and is a key factor for river system health (Delpla et al., 2009). T_w also defines and confines ecological habitats (Isaak et al., 2012; Durance and Ormerod, 2009) and the spread of invasive species (Wenger et al., 2011; Hari et al., 2006). River water is not solely important from an environmental perspective but an important means of production. Especially for energy intensive industries such as power plants, oil refineries, paper or steel mills, river water is an important cooling agent. Its availability is a reason for the choice of their location (Förster and Lilliestam, 2010). In this context, one has to bear in mind, that given a 32 % energy efficiency, 68 % of the energy used in a facility is discharged through the cooling system into the respective stream (Förster and Lilliestam, 2010). This leads to a significant heat load even on large rivers such as the Rhine (IKSR, 2006; Lange, 2009). As a consequence, anthropogenic heat fluxes (heat discharge) can contribute significantly to the heat budget of a river. The natural influences on T_w are: [1] Meteorology, including sensible heat flux, latent heat flux, radiative heat fluxes; [2] Source temperature, which describes the origin of the water, e.g. snow-fed, glacier-fed, groundwater-fed; [3] Hydrology, which influences the water temperature through the amount of water and the flow velocity; [4] Ground heat flux.

T_w can be modeled in two ways, physically or deterministically. A physical T_w model (Sinokrot and Stefan, 1993) parameterizes all fluxes mentioned in [1] and [3], adds anthropogenic heat input and collects the hydrological and source boundary conditions. Each modeled heat flux is then applied to the water mass, initialized with the starting and boundary conditions.

However, it is difficult to get a good estimation of these parameters over the catchment area of a large river. As a consequence, statistical models use air temperature (T_a) as a proxy for sensible, latent and radiative heat fluxes (ground heat flux can be neglected) and establish a $T_a \rightarrow T_w$ relationship through regression. This is a well established method and depending on the complexity, linear or exponential models (Stefan and Preud'homme, 1993; Mohseni et al., 1998; Koch and Grünewald, 2010)

5 are used. Generally the exponential model has advantages due to the better simulation of extremely warm and cold $T_a \rightarrow T_w$ relationships but lacks the clear analytical separation of the different influences to T_w. Markovic et al. (2013) show that between 81 %-90% of the T_w variability can be described by T_a. 9 %-19 % can be attributed to hydrological factors (e.g. discharge). Along the Rhine, up to 12 nuclear power plants (NPP) have caused for decades the largest part of anthropogenic heat input in the river. The nuclear power production increased in the 1970s and 1980s and reached a peak in the mid 1990s. After the

10 Fukushima disaster in 2011, the German government decided to exit from nuclear power production and the first NPPs were shut down. With this political decision a clear drop on nuclear power production was visible, on top of already decreasing production rates. Currently (July 2019) eight NPPs are operational in the catchment area of the Rhine using (partly) river water as cooling agent. In this publication, we hypothesize that, next to environmental factors, this long term decrease in power production together with short term economic changes have an impact on T_w of the Rhine. This impact might be heterogeonous

15 along the river as the location of industry and NPPs is concentrated at several highly industrialized spots.
To revise the hypothesis and asses the varying impact of industry, meteorology and hydrology on the Rhine river temperatures, we run a multiple regression model (Eq. 1) on a T_w time series from 1979 to 2018 measured at four Rhine stations (Basel (CH), Worms (DE), Koblenz (DE) and Cologne (DE)). The period from 1979 to 2018 experienced several changes in anthropogenic heat input to the Rhine catchment area, which makes it an almost ideal scenario to be studied. T_w is regressed with a

20 catchment-wide air temperature T_a and river discharge Q, Eq. 1. a_1, a_2 and a_3 are the resulting regression coefficients.

$$T_w = a_1 + a_2 \cdot T_a + a_3 \cdot Q \tag{1}$$

The origin of water, e.g. ground water, snow melt, glacier melt, is included by the catchment wide approach where T_a at high elevations (e.g. Alps) is also included. Webb et al. (2003) have shown that Q is inversely related to T_w and an important factor (Markovic et al., 2013) in the $T_a \rightarrow T_w$ relationship. Additionally, it functions as measure of how fast a the water mass

25 responds to changes in T_w. Ground heat flux, ground water influx and heat generation due to friction are not included in this model because of the comparable small influence (Sinokrot and Stefan, 1993; Webb and Zhang, 1997).
Using the multiple regression (Eq. 1), we aim to especially investigate the change of a_1 over time, which we call the Rhine base temperature (RBT). This temperature represents the T_w without the influence of meteorology and discharge. RBT is an indicator for industrial heat input and the use of Rhine water as cooling agent. We hypothesize that its long term change is

30 connected with the electricity production of NPPs and its short term variations is connected with overall industrial production and general economic indicators. Using different time series along the Rhine, we investigate where anthropogenic heat fluxes may influence T_w and may lead to an overall heterogeneous warming rate along the Rhine.

name	stream km	time period	important tributary upstream	reference
Cologne	KM 690	1.1.1985-31.12.2018	Mosel	WSA (2019)
Koblenz	KM 550	1.1.1978-31.12.2018	Main	BfG (2019)
Worms	KM 443	1.1.1971-31.12.2018	Neckar	LfU (2019)
Basel	KM 170	1.1.1977-31.12.2018	Aare	BAFU (2019)

Table 1. Lists of monitoring stations used in this study. Column two provides the location as Rhine km. Column three provides the data range. The third column names the important upstream tributary and column four names the reference.

2 Methods

2.1 Water temperature and discharge

We use a data-set of daily averaged T_w and Q from 1979-2018 gathered from different sources (WSA, 2019; BfG, 2019; LfU, 2019; BAFU, 2019). Table 1 lists the respective stations along the Rhine (Col. 1), stream km (Col. 2), data availability

5 (Col. 3), the important tributaries upstream (Col. 4) and the reference (Col. 5). T_w was measured by platinum resistivity sensors (Pt100). The accuracy of theses sensors is commonly ± 0.5 ^{o}C but the precision, which describes the ability to detect temperature changes, is 0.05 ^{o}C.As we focus on the change T_w over time and do not compare the absolute temperature, the accuracy is not essential and the precision is sufficient. Errors inflicted by measuring depth and location in the river are also not influencing the calculation, regarding the aim of this study, as long as the measured T_w is a linearly dependent proxy for

10 the average river temperature. Q is provided as daily averages in m$^3 s^{-1}$ by the reference (Tab. 1 and usually calculated from river stage).

2.1.1 Air temperature

T_a is retrieved from the European Centre for Meridional Weatherforcast (ECMWF) Reanalysis Model ERA5. It provides an hourly time resolution of the 2 m T_a on a $\frac{1}{4}^o$ by $\frac{1}{4}^o$ grid. The data-set is available from 1979-2018. We took the hourly T_a

15 output and calculated a daily mean for each grid point between 1979 and 2018 to fit the time resolution of T_w.

2.2 Catchment Area

The catchment area was calculated using the Hydrosheds database (Lehner et al., 2008). The $\frac{1}{125}^o$ by $\frac{1}{125}^o$ gridded data-set provides information, at each grid point, to which cell the water of a grid cell is drained. Selecting a starting location, e.g. Koblenz at 50.350 ^{o}N and 7.602 ^{o}E it is possible to iteratively calculate all grid points draining into this location. These

20 grid points represent the catchment area of this location, in this case Koblenz. By counting the iteration steps, the distance a water drop travels to reach the monitoring station Koblenz is determined. This was done for each station. Additionally, the accumulation number ACC was calculated. It defines how many cells are draining into a particular cell and is a measure for the size of a river. Finally, a grid, which defines the catchment area, the ACC and the hydrological distance between was established
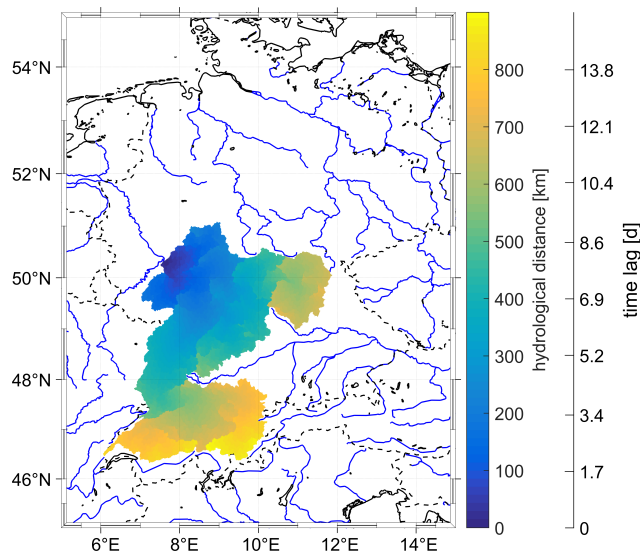
Figure 1. Catchment area of the Koblenz monitoring station. The colors show the hydrological distance between the monitoring station and each grid point of the catchment area. The second y-axis shows the time it takes to flow from a grid point to the monitoring station. The flow speed is 0.733 ms^{-1}

spanning the whole catchment area. Figure 1 shows the catchment area, the distance calculations and the calculated flow time to the Koblenz monitoring station.

2.3 Multiple regression

We use a multiple linear regression to separate the meteorological, hydrological and anthropogenic contributions to the river water temperature. T_w is regressed with T_a and river discharge Q. Their regression coefficients a_2 (T_a slope) and a_3 (Q slope) represent the magnitude of the respective influences. The offset a_1, which we call RBT, combines all other influences, which are mostly from anthropogenic sources.

Instead of using T_a at the monitoring station, we improve Eq. 1 by averaging T_a over the whole catchment area and make T_a time dependent. We call this new parameter catchment temperature T_c. T_c is defined by the location (x,y) and a time lag (Δt).

$$T_w\left(t\right) = a_1 + a_2 \cdot T_c\left(x, y, t + \Delta t\right) + a_3 \cdot Q\left(x_0, y_0, t\right) \tag{2}$$

Time lag and T_c

Linear as well as exponential models have already introduced Δt (Stefan and Preud'homme, 1993; Webb and Nobilis, 1995, 1997) to the $T_a \rightarrow T_w$ relationship. A change in T_a at a location is certainly followed, by a change of T_w to restore equilibrium conditions. The first reason is that the water masses' mixing capability, heat capacity and surface area cause a thermal inertia. Secondly, advection is not taken into account when T_a is measured at the same location and the very same time as T_w. The

Δt [d]	weighing factor	distance from measurement point [km]
0	1	0
-1.0588	0.9412	67
-2.1176	0.8824	113
...	...	...
-18	0	1140

Table 2. This table defines the weighing factors for different time lags and distances from the measurement point. The weight coefficient is linearly correlated to the time lag. Once the time lag is calculated from distance and flow speed (Eq. 5) only the time lag is used in further calculations.

Rhine exhibits current velocities which enable its water to cover significant distances on time scales larger than days. Therefore it is necessary to take advection and the change of T_a, in space and time, during advection into account. Haag and Luce (2008) suggest to use T_a at the same location of the measurement but include the days before to extend the temporal significance. This approach is shown in Eq. 3.

$$T_a = w(t_0) \cdot T_a(x_0, y_0, t_0) + w(t_0 + \Delta t) \cdot T_a(x_0, y_0, t_0 + \Delta t) + w(t_0 + 2 \cdot \Delta t) \cdot T_a(x_0, y_0, t_0 + 2 \cdot \Delta t) ... \tag{3}$$

Time dependent weighing factors $w(t)$ are used to average $T_a(t)$ at different times before the measurement. A linearly decreasing $w(t)$ is used. However, this approach satisfies the idea of thermal inertial but does not include advection. Hence, we extend this idea of a time lagged $T_a(x_0, y_0, t_0 + \Delta t)$ from the location of the T_w measurement to the entire catchment area. All grid points and therefore all possible water streams in the catchment area are assigned with a specific time lag $\Delta t(x, y)$. Using directional discharge maps (Sec. 2.2) and gridded temperature reanalysis data (Sec. 2.1.1), we propose this new 3D (x, y, t) averaging of T_a and call it the catchment temperature T_c, Eq. 4.

$$T_c(t) = \frac{1}{\sum w(\Delta t(x,y))} \sum_{x=1,y=1}^{x=n,y=m} w(\Delta t(x,y)) \cdot T_a(x, y, t + \Delta t(x,y)) \tag{4}$$

$T_c(t)$ is calculated by weighted averaging $T_a(x, y, t)$ over all grid points of the catchment area (x=1,...n y=1,...m) which arrive at the monitoring station at time t. The time lag Δt is the time it takes for a water droplet from a specific grid point in the catchment area to the measurement location. This time can be calculated using the distance s between each grid point in the catchment area and the measurement point and an average flow speed v, Eq. 5. Δt is per definition negative. A comparison of time lag, distance and weighing factor is provided in Tab. 2.

$$\Delta t(x, y) = -\frac{s(x, y)}{v} \tag{5}$$

For reasons of simplification, we did not use a catchment wide hydrological flow model to model the flow speed at every grid point for every hydrological scenario. Therefore we use a constant flow speed of 0.733 ms^{-1}. The weighing factors $w(\Delta t(x,y))$ are shown in Tab. 2. Based on Eq. 4, we calculated the daily T_c for each monitoring station. This temperature represents the meteorological influence all water droplets have experienced on their way to the monitoring station.

Control scenarios

As control scenarios, we introduce two additional weighing coefficients and two different T_c calculations.

The first scenarios (time lag) has a weighing coefficient equal to one for all grid cells, Eq. 6.

$$w\left(\Delta t\left(x,y\right)\right)=1 \qquad T_c\left(t\right)=\frac{1}{n\cdot m}\sum_{x=1,y=1}^{x=n,y=m}T_a\left(x,y,t+\Delta t\left(x,y\right)\right) \tag{6}$$

5   The second scenario (time lag + ACC) is weighing by numbers of grid cells flowing into a particular cell. We call this the accumulation control. The ACC takes into account how much water is accumulated in a specific cell, Eq. 7, which puts more weight on large rivers.

$$w\left(x,y\right)=ACC\left(x,y\right) \qquad T_c\left(t\right)=\frac{1}{\sum ACC\left(x,y\right)}\sum_{x=1,y=1}^{x=n,y=m}ACC\left(x,y\right)\cdot T_a\left(x,y,t+\Delta t\left(x,y\right)\right) \tag{7}$$

The third scenario (no time lag) has a weighing coefficient equal to 1 and does not include a time lag, Eq. 8. It is a plain average

10   over catchment wide T_a at the time of the measurement.

$$w\left(x,y\right)=1 \qquad T_c\left(t\right)=\frac{1}{n\cdot m}\sum_{x=1,y=1}^{x=n,y=m}T_a\left(x,y,t\right) \tag{8}$$

The fourth scenario (T_a at station) uses a single value T_a for each time step at the respective monitoring station, Eq. 9.

$$T_c\left(t\right)=T_a\left(x_0,y_0,t\right) \tag{9}$$

2.4   Nuclear Power Plants

15   The annual electrical power production by NPPs is available from the International Atomic Energy Agency (IAEA) Power Reactor Information System (IAEA, 2019). At most 12 NPPs (1986-1988) were online in the Rhine catchment area. Separate blocks of one NPP are combined. In July 20019 eight were operational. All shutdowns were done in Germany.

From estimates by Lange (2009) and based on personal communication, the heat input by NPPs to the Rhine was calculated for each monitoring station, Fig. 2.

2.4.1   Calculated temperature change

We calculate the expected change in RBT (ΔRBT) due to the change in heat input (ΔHI) by NPPS using the average discharge $\bar{Q}$ and the heat capacity of water c_p, Eq. 10.

$$\Delta RBT=\frac{\Delta HI}{c_p\cdot\bar{Q}} \tag{10}$$

This approach is based on the idea that the heat input of NPPs is essential for the heat budget of the river and significantly

25   alters a_1 as other important influences, such as meteorology (a_2) and hydrology (a_3), are excluded.
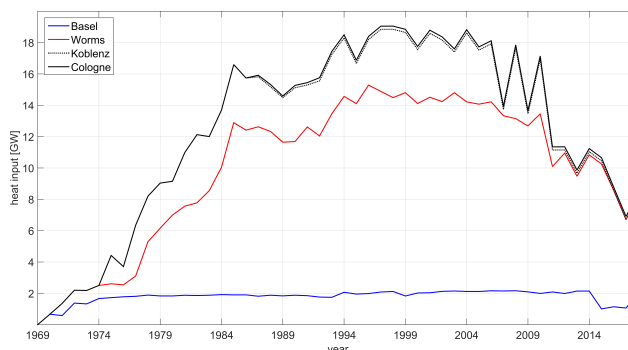
Figure 2. Using the PRIS (IAEA, 2019) database we estimated the heat input by NPPs from 1969 to 2018. This figure shows the total upstream heat input of each monitoring station.

2.5 Gross Domestic Product

The gross domestic product (GDP) for the adjacent German federal states was obtained from VGdL (2019a, b). Due to changes in the calculation method of the GDP before and after the German unification (1991), two separate data-sets are used. For this study only the GDP-change of the secondary sector (construction and production) is used.

5 The RBT, if compared to the GDP, is filtered using a 10th order butterworth bandpass filter. The sampling rate was 12 y^{-1} the cutoff frequencies were 1.1 y^{-1} and 0.05 y^{-1}. This means that a signal with a periodicity larger than 20 y and lower than 0.9 y was dampened. The reason was to make the RBT data comparable to the yearly data of the GDP-change. The low frequency cutoff is canceling long term trends as a GDP-change is only related to the previous year.

3 Results

10 Using the time series of the four monitoring stations and the collected supporting data, we investigate the heterogeneity of the temperature change along the Rhine and the possible anthropogenic influence on T_w.

3.1 Water temperature time series

To investigate the long term change over time, we fitted a time dependent linear function to the time series of T_w and T_a (catchment average) of all four monitoring stations (Basel, Worms, Koblenz, Cologne). The same was done only, when all four

15 monitoring stations had an overlapping data-set (1985-2018). Fig. 3 shows the yearly averaged water temperatures and the linear fits to the two time periods. The fit coefficients and the rate of warming per year are shown in Tab. 3. We also calculated the T_a increase in the catchment area of all monitoring stations. These slopes are shown in column four and five of Tab. 3.

Fig. 3 and Tab. 3 show that the change of T_w is heterogenous along the Rhine. The slope at Basel is approx. six times higher (0.0350 $^{o}Cy^{-1}$) than the one in Cologne (0.0084 $^{o}Cy^{-1}$), comparing only the overlapping data-set. However, during the same

20 period T_a shows similar behavior at these two stations, which is an indication of similar meteorological influence. The T_w
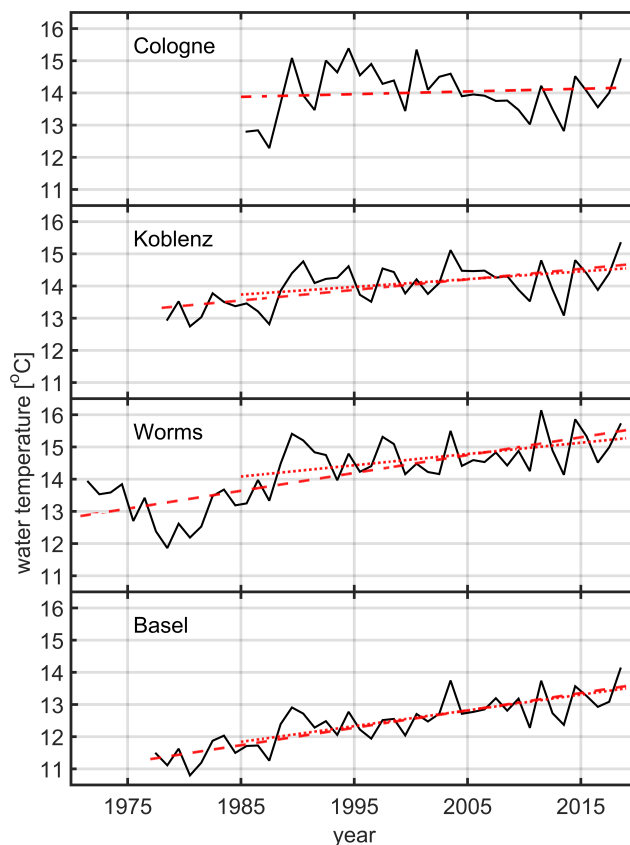
Figure 3. Yearly averages of water temperatures at four monitoring stations (black line). The red dashed line is a fit to the available data-set. The red dotted line is a fit to the overlapping time period.

name	slope T_w whole data-set [^{o}Cy^{-1}]	slope T_w 1985-2018 [^{o}Cy^{-1}]	slope T_a whole data-set [^{o}Cy^{-1}]	slope T_a 1985-2018 [^{o}Cy^{-1}]
Basel	0.0541	0.0489	0.0502	0.0497
Worms	0.0554	0.0350	0.0503	0.0481
Koblenz	0.0328	0.0240	0.0518	0.0481
Cologne	0.0084	0.0084	0.0497	0.0497

Table 3. Slope of the linear fits to the daily temperature data. The second column is a fit to the available T_w data-set. The third column is a fit to the overlapping T_w data-set from 1985-2018. The fourth column is the rate of T_a increase in the respective catchment area during the whole data-set. The fifth column is the rate of T_a increase in the respective catchment area from 1985-2018.

warming rate from 1985-2018 for Worms and Koblenz are in between those from Cologne and Basel. These two stations show similar T_a warming rates when comparing to Basel and Cologne. Generally, the T_a warming rates are less than 5 % different. We hypothesize that meteorological conditions are not the reason for this difference. Meteorological differences should be

	Basel	Worms	Koblenz	Cologne
Time lag+weight	1.71	1.35	1.27	1.65
Time lag	1.68	1.32	1.18	1.50
Time lag+ACC	1.72	1.37	1.39	1.72
No time lag	2.48	2.43	2.37	2.56
T_a at station	2.66	2.55	2.63	2.85

Table 4. Root mean square errors [^{o}C] for five scenarios. The model is applied over the whole data-set. The first row is the scenarios used for all other results.

visible in the T_a warming rate, which is not the case in this data-set. Therefore, we applied the regression model (Eq. 2) to investigate this pattern of T_w along the Rhine river.

Comparing this data-set to a study by Webb (1996) shows that the T_w increase is relatively high in comparison the 20th century results. Webb (1996) reported a 1 ^{o}C warming rate for an average European river during the 20th century ($\cong$ 0.01 ^{o}Cy^{-1}).
5   Using the warming rate of this study, only Cologne fits this projection. Basel and Worms show a five to six times higher and Koblenz a three times higher warming rate.

3.2   RBT, long and short term trends

We fitted the multiple regression model (Eq. 2), using T_c and Q to T_w of each monitoring station. Afterwards, we recalculated T_w using the regression coefficients a_1, a_2 and a_3. From the comparison between the modeled and measured T_w, we calculated
10   the root mean square error (RMSE) and the Nash-Sutcliff coefficient (NSC) for each monitoring station (Tab. 4 and 5).

As a control, to support the introduction of weighing coefficients and a catchment-wide time lag, we used the four scenarios from Sec. 2. Tab. 4 and 5 show the RMSE and NCS values for all scenarios. The lowest RSME is 1.18 ^{o}C for the time lag (row two) at the Koblenz station. At this location also the largest NCS of 0.96 appears at two scenarios, time lag and time lag+weight. It is evident that the two scenarios with time lag have a lower RMSE (below 1.75 ^{o}C) than the two scenarios
15   without a time lag (above 2.4 ^{o}C). The same trend holds for NCS where the time lag scenarios are above 0.91 and the other two are below 0.86.

We think that the use a catchment wide time lag improves the quality of the multiple regression analysis and is a significant improvement to $T_a \rightarrow T_w$ based modelling. It is interesting that a time (or distance) dependent weighing factor does not improve the model output. This implies that even the furthest and oldest T_a influences on T_w are still carried as information by
20   a small temperature difference in the water mass.

3.3   Rhine base temperature

From the multiple regression in Sec. 3.2 we obtained the coefficients a_1-a_3 (Eq. 2). The magnitudes a_2 and a_3 relate to the influences by meteorology and hydrology (discharge). a_1 is the RBT, which is an indicator for the anthropogenic impact on T_w. We use the RBT to explain differences in the T_w warming rates of Tab. 3.

	Basel	Worms	Koblenz	Cologne
Time lag+weight	0.91	0.95	0.96	0.94
Time lag	0.92	0.95	0.96	0.95
Time lag+ACC	0.91	0.95	0.95	0.93
No time lag	0.82	0.84	0.86	0.84
T_a at station	0.79	0.82	0.82	0.80

Table 5. NSC for five scenarios. The model is applied over the whole data-set. The first row is the scenarios used for all other results.
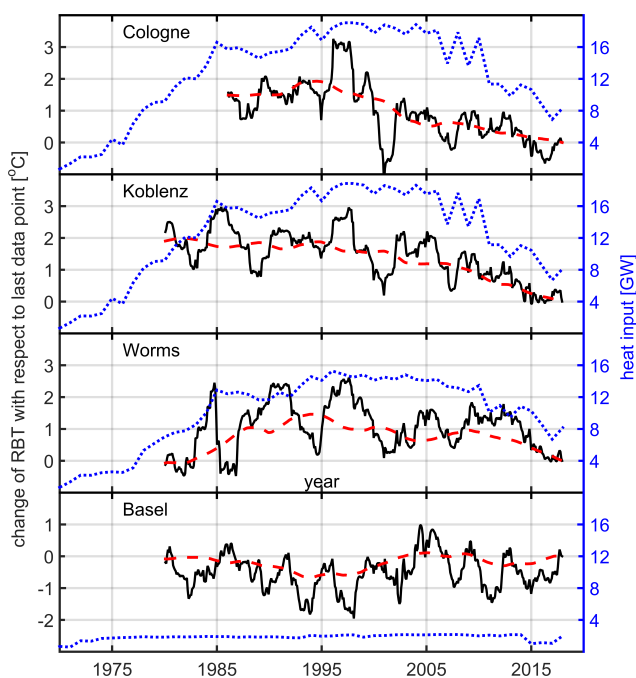
Figure 4. RBT from four monitoring stations (black solid line). The red dashed line is a four year running mean. The blue dotted line is the upstream heat input by NPPs (Sec. 2.4).

To point out changes over time, we regressed a two year segment of the T_w time series and used a step size of one month to create a RBT time series over the available data-set. As the absolute RBT does not have a distinct meaning, only the changes of RBT over time are shown in Fig. 4. We subtracted the last data point of each time series from the rest of the data and show the change of RBT vs time and a four-year running mean. The heat input by NPPs is shown as a dotted blue line with the y-axis on the right hand side.

name	period	ΔRBT from data-set	ΔRBT from Eq. 10	ΔGW
Basel	2008-2017	-0.08	0.04	0.17
Worms	1996-2017	1.26	1.18	7.14
Koblenz	1999-2017	1.55	1.45	10.5
Cologne	1998-2017	1.2	1.52	10.7

Table 6. The table shows the change of RBT (column 3) in the period given in column 2. The calculated temperature change (column 4) and the change in HI by nuclear power plants (column 5) are also provided.

Long term trend

In this study long term trends occur on time scales of decades. This time scale is on one hand small enough to have significance in this 40 year data-set and on the other hand covers the increase and decrease of nuclear power production.

The heat input by NPPs and the four-year running mean RBT follow a similar trend. After the maximum of heat discharge by

5 NPPs between 1996-1998, the heat input as well as the RBT of Worms, Koblenz and Cologne decline. At Basel the RBT as well as the heat input stay comparably constant. To investigate these similar trends we calculate ΔRBT, using Eq. 10, at every station and compare it to the ΔRBT from the measured T_w, Tab. 6.

At Basel, both simulated and calculated RBT changes are negligible due to the lack of change in HI. At all other stations, the change in HI is reflected in the change of RBT. The maximum difference between simulation and calculation is 0.32 ^oC.

10 The change in nuclear power production over the a time period of 30 years or more can explain changes and heterogenous warming rates of T_w along the Rhine river. NPPs may also impact T_w at much shorter timer scale but do not seem,to our best knowledge, to change their power output accordingly.

Short term trend

Short term changes (< 5 y) in RBT (Fig. 4) are not influenced by the overall heat in put from NPPs, as they change production

15 at longer time scales, but rather by local industrial conditions, which could also include fossil fuel power plants.

For Basel, we hypothesize that the varying, but on average constant, RBT is influenced by alpine lakes. Lakes and reservoirs are to some extend decoupled from the $T_a \rightarrow T_w$ relationship (Erickson and Stefan, 2000). The upper layer (epilimnion) closely follows T_a and the temperature of the larger volume underneath is usually more stable and colder (summer) or warmer (winter). The stratification plays an important role in the outflow temperature of a lake. Another indication, for the weakness of

20 the $T_a \rightarrow T_w$ model, is that the regression model has its largest RMSE (1.71 ^oC) at this station regarding the time lag scenarios. For all other stations, we hypothesize that local production facilities and their heat input into the Rhine are responsible for the short term changes. Therefore we compare the RBT time series to economic data. Fig. 5 shows the comparison of RBT (black line, one year running mean) vs the changes in the GDP (blue line). A discontinuity in the GDP at 1991 is visible, due to the German reunification, when the calculation method of the GDP changed. Therefore they are plotted as separate lines.

25 For Worms (Fig. 5, bottom panel) we added the change of turnover of the BASF company (red dashed line (AG, 1989)). Its
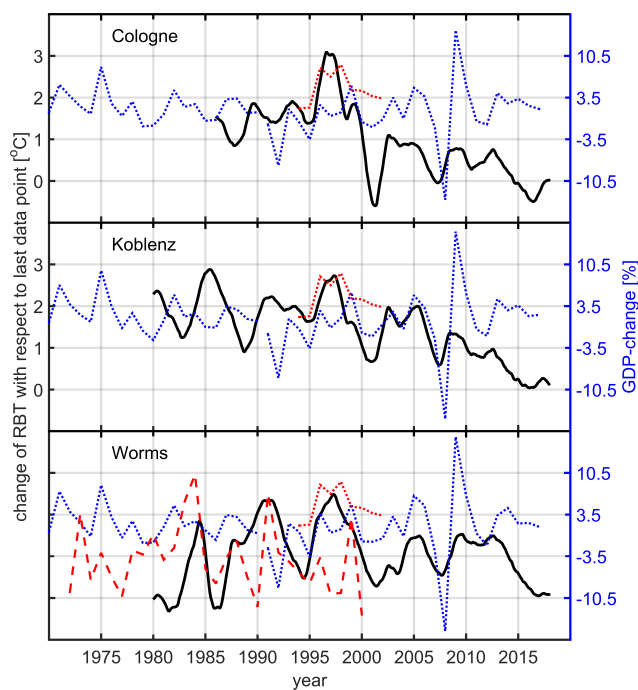
Figure 5. The change of RBT (black solid line) at three monitoring stations (Colgone, Koblenz, Worms). The blue dashed line is the GDP-change of the adjacent federal states. To explain trends during two time periods the red dashed line, which is the turnover of the BASF company, and the red dotted line, production rate of the oil refineries, are added.

production facility is located 12 km upstream (km 431) from the Worms station. In 1985, although the change in GDP does not indicate a large RBT change, a significant RBT decrease is visible. This is backed by a turnover decrease in 1985 and 1986. After the German reunification 1991, a negative GDP change (recession) is evident. This followed by a by a BASF turnover decline as well as a decrease in RBT. After that, the RBT follows the up and down movements of the GDP, so does the BASF
5   turnover (only shown until 2000). Especially the economic events such as the burst of the dot-com bubble (early 2000s) and the mortgage crisis (2008) are visible in the RBT and the GDP, when a decrease of both parameters followed.

Before 1990, the RBT at Koblenz does not follow the GDP trend and shows a rather anti-cyclic behavior, which can not be explained yet. After 1991, the RBT follows the general trend of the GDP but does not seem to be strongly influenced by the recession after the German unification. Again, economic events such as the burst of the dot-com bubble (early 2000s) and the
10   mortgage crisis (2008) have influence on the RBT.

The RBT at Cologne does not seem to be strongly influenced by the recession connected to the German reunification, but after 1999 the RBT follows the up and down trends of the GDP.

For all monitoring stations, we added a red dashed line between 1995 and 1999. This dashed line indicates the production rate of German oil refineries (MWV, 2003). From 1995 to 1999 German refineries ran at full capacity level (100%). Usually
15   the capacity levels do not exceed 90%. The increase in production is clearly visible in the RBT of Cologne, where a large oil

name	time-lag + weigh	time-lag	significance
Worms	0.42	0.47	p<0.05
Koblenz	0.52	0.44	p<0.05
Cologne	0.44	0.39	p<0.05

Table 7. Spearman's rank correlations between RBT and GDP-Change for two scenarios. The last column shows the significance

refinery is located 19 km upstream at km 671 (Rheinland refinery). RBT at Worms and Koblenz could be influenced by the output of the refinery next to Karlsruhe at km 367 (Mineraloelraffinerie Karlsruhe).

Correlation

We correlate the GDP-change to the filtered RBT signal. It is noticeable that we shifted the GDP-change 480 days to the past

5   to get matching trends. This means that a change in RBT or anthropogenic heat input appears 480 days earlier than in the GDP calculation. The shift could be caused by two reasons: [1] We are using the GDP difference of two consecutive years, which has a significance at a point of time within these two years. [2] The GDP could be lagging behind the real economic situation, in this case the industrial production. (Yamarone, 2012) claims that GDP is a coincident economic indicator similar to industrial production. However, he uses quarterly GDP calculations vs our annual data. The quaterly data-set could be reacting faster to

10   changes. A second thought is that he compares industrial production calculations, which is an economic index, to GDP (another economic index). We have basically real time data from the industrial heat input into the river. This shift was not done in Sec. 3.3 because a shift of 1.5 y on a 40-year time scale is negligible.

Tab. 7 shows the Spearman's rank correlation coefficients of Worms, Koblenz and Cologne for the time-lag and the time-lag + weight scenarios. All correlations are positive and significant (p<0.05). The correlation of the RBT data-set with weighing is

15   slightly higher (except for Worms) than those from equally weighted T_a. The correlation in Koblenz is the highest. Fig. 6 shows the filtered RBT signal vs the GDP-change at the three monitoring stations. Most of the time the change in filtered and shifted RBT is coincident with the GDP-change. The RBT peak from 1995-1998 is not very well represented by the GDP-change, which has already been discussed in context of Fig. 5.

4   Conclusions

20   We introduce a new catchment-wide air temperature T_c, which decreases the RMSE (Tab. 5 and 4) in a $T_a \rightarrow T_w$ regression. T_c is an average of all T_a across the catchment including the improvement by using a the time lag for each grid point according to the hydrological distance and flow speed. This time lag is an indicator when a measured water droplet was at a certain grid cell in the catchment area. As a result, one can get a better estimate which T_a a water droplet experienced on its way to a monitoring station and better linear $T_a \rightarrow T_w$ estimates. An improvement in the $T_a \rightarrow T_w$ relationship makes analysis,

25   reanalysis and forecast of T_w easier as T_a data is readily available. Still a sufficient time-series of T_w is required. The linear relationship is simpler than a full physical model which needs all meteorological fluxes as parameters.
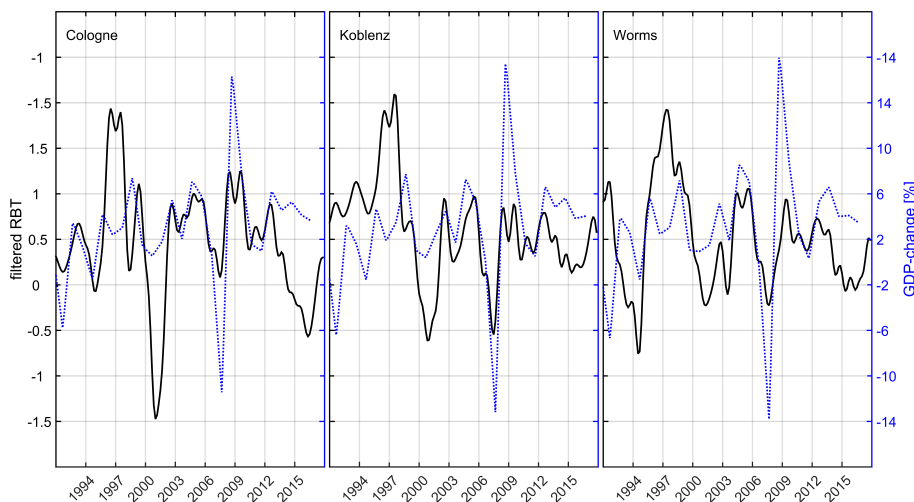
Figure 6. The three panels show the filtered RBT signal (black solid) and the GDP change (blue dashed) at the Cologne, Koblenz and Worms.

This a case study for the Rhine catchment area but the model can be used in any river system around the globe. Catchment area data and reanalysis T_a data are globally available. Morrill Jean et al. (2005) show a linear $T_a \rightarrow T_w$ relationship for 43 rivers with various catchment areas in the subtropics. This could indicated that this case study of the Rhine can be applied globally. There is a lack of studies on the $T_a \rightarrow T_w$ relationship in the tropics, where precipitation and extreme evens, such as monsoon,

5 could complicate this relationship. Future calculations could be coupled with catchment wide hydrological models to improve the accuracy of the time lag.

Using T_c we regress four T_w time series (Basel, Worms, Koblenz and Cologne) along the Rhine. The offset in the this regression a_1, which we call RBT and its change over time is an indicator for anthropogenic heat input. The RBT can be correlated with long term economic changes such as the decrease of nuclear power production as well as short term economic events. We

10 showed that change in production rates (oil refineries), a change in GDP can influence the RBT and therefore the Rhine water temperature. Also a statistical correlation supports the connection between RBT and GDP. This case study could be on one hand a tool for understanding the long term consequences of industrial water use and on the other hand a verification tool for reported heat input. Germany has a rigorous reporting system on cooling water use. However, other countries could check if industrial heat input is in accordance with legislative guidelines.

15 (Hardenbicker et al., 2016) estimate, using a physical model (QSim), that between the reference period of 1961-1990 and the near future 2021-2050 the mean annual T_w of the Rhine could increase by 0.6 ^{o}C-1.4 ^{o}C. This trend can be supported by our historical data, however they use a constant anthropogenic heat input. Differences along the Rhine might be introduced by a change in anthropogenic heat input. The difference of the T_w warming rate between Basel and the other monitoring stations can be explained by the change in nuclear power production and the influence of general industrial production. This could mean

20 that with rising T_a and the linear correlation between $T_a \rightarrow T_w$, industrial production and power production have to be more closely connected with river water temperature management. For the Rhine river we find a decreasing, except for Basel, RBT.
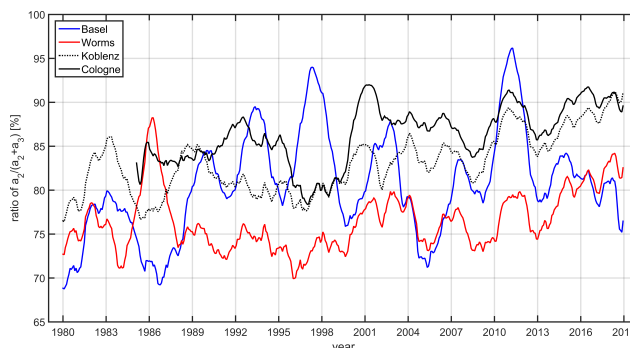
Figure A1. The relative contribution of a_2 to the variation in T_w at the four monitoring stations.
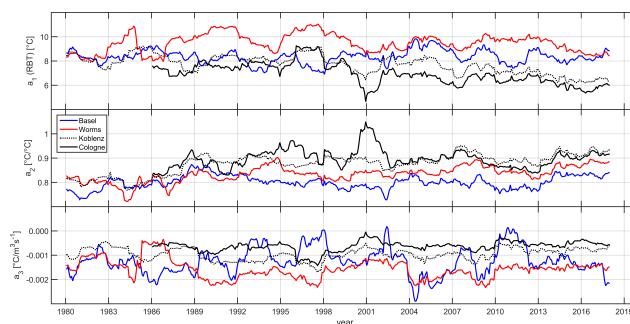
Figure A2. The relative contribution of a_2 to the variation in T_w at the four monitoring stations.

However, other river catchment areas with growing energy intensive industries could experience a larger warming rate than it is caused by the general increase of T_a experiencing all consequences for the physical, chemical and biological processes.

Appendix A: Regression coefficients

In Sec. 3.2 regression coefficients a_{1-3} were calculated by regressing T_w by T_c and Q. The regression was done on a two-year window with a step size of one month. Fig. A1 shows the evolution of the regression coefficients at all four monitoring stations for the Time-lag+ weight scenario, as an example. Fig. A2 shows a_2 (meteorology) in relation to both environmental influences a_2+a3. The y-axis percentage gives an indication, how much influence a_2 has on the variations of T_w. The remaining percentage to 100 % can be attributed to a_3 (hydrology).

name	country	river	conversion factor	const. heat input
Beznau I+II	CH	Aaare	3	N/A
Biblis I+II	DE	Rhine	2	N/A
Cattenom I-IV	DE	Mosel	N/A	200 MW
Fessenheim I+II	FR	Rhine	3	N/A
Goesgen	CH	Aare	N/A	50 MW
Grafenrheinfeld	DE	Main	N/A	200 MW
Leibstatt	CH	Rhine	N/A	50 MW
Muehleberg	CH	Aare	3	N/A
Neckarwestheim I+II	DE	Neckar	1	N/A
Obrigheim	DE	Neckar	3	N/A
Philippsburg I+II	DE	Rhine	1	N/A

Table B1. NPPs included in this manuscript. The coversion factor describes the conversion from electrical power generation to heat input. If cooling towers are installed a constant heat input was used based on Lange (2009).

Appendix B: Nuclear Power Plants and Output

Following NPPs were included in the heat input calculation(Tab. B1). The conversion factor is used to convert electrical produced power to heat input. NPPs with an exclusive river water cooling system have a conversion factor of three, which is based on the power efficiency of electricity generation. Other factors are estimated depending on the used cooling system.

5   *Author contributions.* AZ and LD did the study concept and design. AZ collected the data, developed the model, analyzed the data and wrote the manuscript in consultation with LD. LD provided critical feedback and helped shape the research.

Competing interests. The authors declare no competing interests

Acknowledgements. We acknowledge all data providers for their help. The German Federal Ministry of Transport and Digital Infrastructure for founding the Federal Institute of Hydrology and therefore making this work possible

References

AG, B.: BASF Geschaeftsbericht, BASF AG Oeffentlichkeitsarbeit und Marktkommunikation 67056 Ludwigshafen Deutschland, 1989.

BAFU: Water temperature and discharge Basel, Bundesamt fuer Umwelt BAFU Abteilung Hydrologie, https://www.bafu.admin.ch, 2019.

BfG: Water temperature and discharge Koblenz, Bundesanstalt fuer Gewaesserkunde, Am Mainzer Tor 1, 56068 Koblenz, www.bafg.de, 2019.

Delpla, I., Jung, A.-V., Baures, E., Clement, M., and Thomas, O.: Impacts of climate change on surface water quality in relation to drinking water production, Environment International, 35, 1225–1233, http://www.sciencedirect.com/science/article/pii/S0160412009001494, 2009.

Durance, I. and Ormerod, S. J.: Trends in water quality and discharge confound long-term warming effects on river macroinvertebrates, Freshwater Biology, 54, 388–405, https://doi.org/10.1111/j.1365-2427.2008.02112.x, 2009.

Erickson, T. R. and Stefan, H. G.: Linear Air/Water Temperature Correlations for Streams during Open Water Periods, Journal of Hydrologic Engineering, 5, 317–321, https://doi.org/10.1061/(ASCE)1084-0699(2000)5:3(317), https://ascelibrary.org/doi/abs/10.1061/%28ASCE%291084-0699%282000%295%3A3%28317%29, 2000.

Förster, H. and Lilliestam, J.: Modeling thermoelectric power generation in view of climate change, Regional Environmental Change, 10, 327–338, https://doi.org/10.1007/s10113-009-0104-x, 2010.

Haag, I. and Luce, A.: The integrated water balance and water temperature model LARSIM-WT, Hydrological Processes, 22, 1046–1056, https://doi.org/10.1002/hyp.6983, 2008.

Hardenbicker, P., Viergutz, C., Becker, A., Kirchesch, V., Nilson, E., and Fischer, H.: Water temperature increases in the river Rhine in response to climate change, Regional Environmental Change, 17, 299–308, https://doi.org/10.1007/s10113-016-1006-3, 2016.

Hari, R. E., Livingstone, D. M., Siber, R., Burkhardt-Holm, P., and Guettinger, H.: Consequences of climatic change for water temperature and brown trout populations in Alpine rivers and streams, Global Change Biology, 12, 10–26, https://doi.org/10.1111/j.1365-2486.2005.001051.x, 2006.

IAEA: Power Reactor Information System (PRIS), Web, pris.iaea.org/pris/, 2019.

IKSR: Vergleich der Waermeeinleitungen 1989 und 2004 entlang des Rheins, IKSR-Bericht, 2006.

Isaak, D. J., Wollrab, S., Horan, D., and Chandler, G.: Climate change effects on stream and river temperatures across the northwest U.S. from 1980–2009 and implications for salmonid fishes, Climatic Change, 113, 499–524, https://doi.org/10.1007/s10584-011-0326-z, https://doi.org/10.1007/s10584-011-0326-z, 2012.

Koch, H. and Grünewald, U.: Regression models for daily stream temperature simulation: case studies for the river Elbe, Germany, Hydrological Processes, 24, 3826–3836, https://doi.org/https://doi.org/10.1002/hyp.7814, 2010.

Lange, J.: Waermelast Rhein, Bund fuer Umwelt und Naturschutz Deutschland, www.bund-rlp.de/, 2009.

Lehner, B., Verdin, K., and Jarvis, A.: New Global Hydrography Derived From Spaceborne Elevation Data, Eos, Transactions American Geophysical Union, 89, 93, https://doi.org/10.1029/2008eo100001, https://doi.org/10.1029/2008EO100001, 2008.

LfU: Water temperature and discharge Worms, Landesamt fuer Umwelt Rheinland-Pfalz, https://lfu.rlp.de/, 2019.

Markovic, D., Scharfenberger, U., Schmutz, S., Pletterbauer, F., and Wolter, C.: Variability and alterations of water temperatures across the Elbe and Danube River Basins, Climatic Change, 119, 375–389, https://doi.org/10.1007/s10584-013-0725-4, 2013.

Mohseni, O., Stefan, H. G., and Erickson, T. R.: A nonlinear regression model for weekly stream temperatures, Water Resources Research, 34, 2685–2692, https://doi.org/10.1029/98WR01877, 1998.

Morrill Jean, C., Bales Roger, C., and Conklin Martha, H.: Estimating Stream Temperature from Air Temperature: Implications for Future Water Quality, Journal of Environmental Engineering, 131, 139–146, https://doi.org/10.1061/(asce)0733-9372(2005)131:1(139), https://doi.org/10.1061/(ASCE)0733-9372(2005)131:1(139), 2005.

MWV: Mineraloel und Raffinerien, Mineraloelwirtschaftsverband e.V., 2003.

5 Sinokrot, B. A. and Stefan, H. G.: Stream temperature dynamics: Measurements and modeling, Water Resources Research, 29, 2299–2312, https://doi.org/10.1029/93WR00540, 1993.

Stefan, H. G. and Preud'homme, E. B.: STREAM TEMPERATURE ESTIMATION FROM AIR TEMPERATURE, Journal of the American Water Resources Association, 29, 27–45, https://doi.org/10.1111/j.1752-1688.1993.tb01502.x, 1993.

VGdL, A.: Bruttoinlandsprodukt, Bruttowertschoepfung in den Laendern der Bundesrepublik Deutschland, Revision 2014, www.statistik-10 bw.de/VGRdL, 2019a.

VGdL, A.: Rueckrechnungsergebnisse fuer das frueherer Bundesgebiet, Revision 2005, www.statistik-bw.de/VGRdL, 2019b.

Webb, B. W.: Trends in stream and river temperature, Hydrological Processes, 10, 205–226, https://doi.org/10.1002/(SICI)1099-1085(199602)10:2<205::AID-HYP358>3.3.CO;2-T, 1996.

Webb, B. W. and Nobilis, F.: Long term water temperature trends in Austrian rivers, Hydrological Sciences Journal, 40, 83–96, 15 https://doi.org/10.1080/02626669509491392, https://doi.org/10.1080/02626669509491392, 1995.

Webb, B. W. and Nobilis, F.: LONG-TERM PERSPECTIVE ON THE NATURE OF THE AIR–WATER TEMPERATURE RELATIONSHIP: A CASE STUDY, Hydrological Processes, 11, 137–147, https://doi.org/10.1002/(SICI)1099-1085(199702)11:2<137::AID-HYP405>3.0.CO;2-2, 1997.

Webb, B. W. and Zhang, Y.: Spatial and seasonal variability in the components of the river heat budget, Hydrological Processes, 11, 79–101, 20 https://doi.org/10.1002/(SICI)1099-1085(199701)11:1<79::AID-HYP404>3.0.CO;2-N, 1997.

Webb, B. W., Clack, P. D., and Walling, D. E.: Water-air temperature relationships in a Devon river system and the role of flow, Hydrological Processes, 17, 3069–3084, https://doi.org/10.1002/hyp.1280, 2003.

Wenger, S. J., Isaak, D. J., Dunham, J. B., Fausch, K. D., Luce, C. H., Neville, H. M., Rieman, B. E., Young, M. K., Nagel, D. E., Horan, D. L., and Chandler, G. L.: Role of climate and invasive species in structuring trout distributions in the interior Columbia River Basin, 25 USA, Canadian Journal of Fisheries and Aquatic Sciences, 68, 988–1008, https://doi.org/10.1139/f2011-034, 2011.

WSA: Water temperature and discharge Cologne, Wasserstraßen- und Schifffahrtsamt Duisburg-Rhein, http://www.wsa-duisburg-rhein.wsv.de, 2019.

Yamarone, R.: Indexes of Leading, Lagging, and Coincident Indicators, John Wiley and Sons, Inc., https://doi.org/10.1002/9781118532461.ch2, 2012.